This article has been accepted for publication in IEEE Transactions on Industry Applications. This is the author's version which has not been fully edited and content may change prior to final publication. Citation information: DOI 10.1109/TIA.2023.3234232

A General Methodology for Short-circuit Calculations in Hybrid AC/DC Microgrids

Salvatore Favuzza
Senior Member, IEEE
Engineering Department
University of Palermo
salvatore.favuzza@unipa.it

Massimo Mitolo
Fellow, IEEE
School of Integrated Design, Engineering and Automation
Irvine College
mmitolo@ivc.edu

Salar Moradi
Engineering Department
University of Palermo
salar.moradi@community.unipa.it

Rossano Musca
Senior Member, IEEE
Engineering Department
University of Palermo
rossano.musca@unipa.it

Gaetano Zizzo
Senior Member, IEEE
Engineering Department
University of Palermo
gaetano.zizzo@unipa.it

***Abstract* – In this paper, the issues related to short-circuit calculations in hybrid AC/DC microgrids are discussed. The reference standard for short-current calculations in DC systems is the IEC 61660, which provides a mathematical formulation of the problem. The standard only includes radial DC grids and does not consider a more complex system, such as meshed DC systems or a hybrid AC/DC microgrid. This paper proposes a generalized approach that can be used independently of the characteristics of the hybrid system. The proposed approach is applied to four test microgrids with different distributed sources and number of nodes and the results are compared with those obtained simulating the same grids with Neplan 360®.**

***Index Terms*—AC/DC Microgrids, Short-circuit, Fault calculation, hybrid systems.**

I. Introduction

Over the past decade, the concepts of DC and hybrid AC/DC microgrids have become a popular topic among engineers, fueling the debate on pros and cons of transforming an AC distribution system into a DC. This matter has been examined from different perspectives and by considering structural, design, and operational concerns.

As an example, in [1] and [2], the authors present a comprehensive review of power architectures, applications, and standardization issues, control strategies and stabilization techniques for DC microgrids. The voltage control issue is discussed in [3], where the authors propose an energy management strategy of active distribution systems with a grid-connected DC microgrid, as well as for an isolated DC microgrid with hybrid energy resources. In [4], a power architecture for residential buildings consisting in a multilevel DC microgrid is presented, together with a method for maximizing the energy efficiency of parallel DC/DC converters. In [5], a microgrid based on solar PV-battery energy storage with a multifunctional voltage source converter is presented. In [6], a new and more flexible architecture for hybrid AC/DC microgrids with a multi-port interconnected converter is proposed. Finally, in [7] and [8] a simulation analysis for assessing the reliability of AC/DC hybrid microgrids is performed on four test grids and some system's indicators are assessed.

A. Motivation of the research and research gap

In this context, the topic of calculating short-circuit currents in DC networks is of interest. The standard IEC 61660 [9] proposes a short-circuit current calculation methodology but given the age of this document the most recent developments in technology and, among other things, the simultaneous presence of AC and DC sources, are not considered. The methodology proposed in this paper tries to fill this research gaps due to the increasing importance that hybrid AC/DC systems are gaining in modern distribution grids.

B. Background and related works

With the aid of a power grid simulation software, some authors have tried to overcome the limitations of [9] and have proposed improvements based on simulation results. In[10], the authors develop an original package of programs used for the analysis and rating of DC protective devices in power systems. In [11]-[12], two different modeling approaches to evaluate DC-side short-circuit currents in DC distribution systems fed by rectifiers are presented and validated by a time-domain simulation. The above-cited works present useful formulae that could be integrated in the IEC 61660 approach when DC distribution systems are applied to microgrids operating in island mode. Reference [13] presents an algebraic model to approximate the DC short-circuit current contribution of converters without DC fault ride-through capability. In [14], the authors analyze the limits in the application of the IEC 61660 standard to HVDC systems. In [15], the author shows that the equations of the IEC 61660 standard, originally for low-voltage (LV) systems, can also be applied to medium voltage (MV) DC networks and discusses some limitations of the standard. In [16], HVDC systems in short-circuit conditions are studied in the case of dual inverters with dual DC-link; however, the authors, although providing an interesting description of the control system, do not consider these devices in a more general methodology for calculating DC short-circuit currents. The research work in [17] proposes a fault current calculation method for DC railways. The paper presents a method to model in Matlab/Simulink railway substations, trackside paralleling huts, wayside energy storage

devices, track feeders (positive and negative), overhead contact systems, running rails, and rail-to-earth resistance. The results of the short-circuit calculation are compared with those obtained from the simplified formulas of the international standard EN 50123-1 standard for DC railway systems [18]. In [19], the authors propose the wavelet transform to extract high-frequency components of fault currents to identify internal and external faults in VSC-HVDC grids. In addition, to design a protection circuit breakers in DC side, authors use the instantaneous voltage polarity difference of the current limiting reactor to determine the fault direction.

Some further steps in the simulations of DC short-circuits are done in [20] and[21]. In the first paper, the authors present an approach and some formulae for short-circuit calculation in a DC system in the case of line-to-line and line-to-ground faults and validate the results with Matlab/Simulink. In the second paper, a mathematical model and the related experimental validation are presented for short-circuit calculations in DC grids supplied by hybrid AC/DC power supply generators. The research work in [22] tries to distinguish steady-state, transient and fault operation in low voltage DC microgrids supplied by PV and battery storage systems. The proposed algorithm calculates residual current in voltage source converters and load branches, while not consider the effect of generation units. The models proposed in [23]-[24] are compared to simulation results. The prior adopted a mathematic model to calculate short-circuit current in multi-terminal DC grid using simplified converters and overhead line circuits, and the second one calculates short circuit current in HVDC systems considering IEC 61660. In [25], the authors model a DC-side bipolar fault current in steady-state stage for modular multilevel converters connected to AC system. Finally, in [26], an approach to extend the IEC 61660 standard to meshed systems is proposed.

All the above-mentioned works deals with the modelling of specific components of the DC system, with the dynamic behaviour of the system during the fault or propose methods that are used for DC grids with a single source.

C. *Main contribution of the proposed work*

In this context, this paper proposes a generalized approach that can be used for calculating AC/DC short-circuit currents in hybrid AC/DC microgrids, independently of the characteristics of the hybrid system. The methodology is based on the main equations of the IEC 61660 standard, employed for the calculation of equivalent resistances for a matrix formulation of the problem. This methodology can be applied to both radial and meshed structures since, as it is further clarified in this paper, meshed structures can also be reduced to simpler radial configurations. To demonstrate the robustness of this proposed method, two test microgrids are examined and the results are compared with those obtained with the modelling software Neplan 360®.

D. *Structure of the paper*

The rest of the paper is organized as it follows:

- Section II presents the proposed methodology and contains several references to the original IEC 61660 standard;
- Section III presents various case studies defined for testing the proposed methodology;
- Section IV reports the conclusions of the work.

II. METHODOLOGY

Fig. 1 shows a generic topology of a DC microgrid with N buses, loads, and sources. Each DC source can be a rectifier, a battery energy storage system (BESS), a capacitor, or a DC motor (Fig. 2). Other types of DC sources, such as fuel cells or photovoltaic systems, are not considered because the IEC 61660 standard does not provide any guidance for calculating the short-circuit current in the presence of such elements.

$$[I_F] = [G_{SC}][U_0] - [G_{SC}][U_F] \quad (1)$$

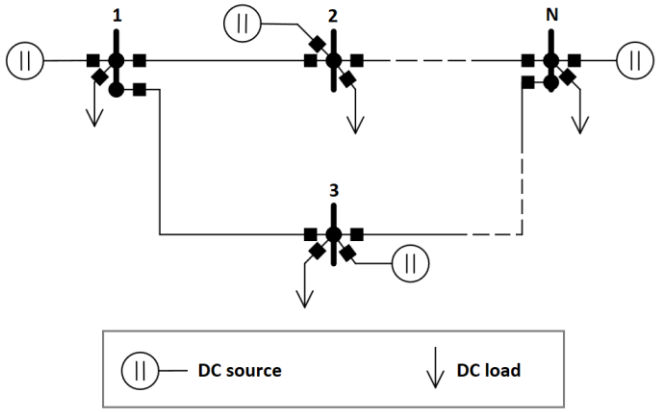

Fig. 1. Generic representation of a DC microgrid with N buses.

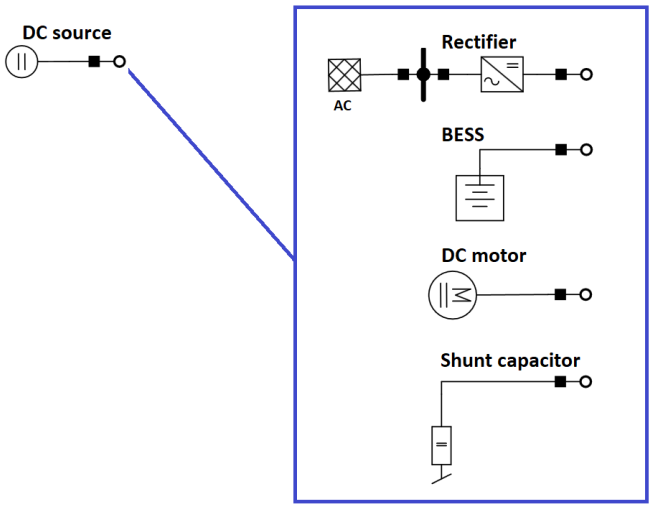

Fig. 2. DC sources considered in the study according to IEC 61660.

Rectifiers are located at the connection points between DC microgrids and AC grids, and their presence will be used to include the fault current contribution of the main AC system into the calculation.

The steady-state short-circuit current calculation at a generic i^{th} bus of the DC microgrid in Fig. 1 is performed by calculating the short-circuit conductance matrix $[G_{SC}]$ [26]-[27]. According to this method, the short-circuit current is found solving the matrix equation:

Where $[I_F]$ is a vector that has all null elements except the ith element, which is the fault current $I_{F,i}$ at the i^{th} node, $[U_0]$ is a vector whose elements are the voltages at the nodes of the DC microgrid, which are assumed to be equal to the rated voltage of the system, or to the pre-fault voltages obtained by means of the load flow analysis of the microgrid. Finally, $[U_F]$ is a vector whose elements are the voltages at the nodes of the DC microgrid during the fault. The i^{th} element of $[U_F]$ is set to zero in the case of a bolted short-circuit fault (i.e., zero impedance), all other elements, including the fault current, are the unknowns of the system. Equation (1) represents, therefore, a system with N equations and N unknowns (1 current and N-1 bus voltages). The diagonal element G_{kk} of the conductance matrix $[G_{SC}]$ is obtained as the sum of all conductances of all elements connected to the k^{th} bus. The extra-diagonal element G_{kh} of the matrix is the opposite of the sum of all conductances of all elements connecting buses k and h. For calculating the contribution of a DC source to a generic G_{kk} element, the expressions reported in the standard IEC 61660 are used. A more detailed description of the IEC 61660 approach is not in the scope of this paper and can be found both in [10] and in [15].

In the case of a BESS, the equivalent resistance of the source is given by:

$$R_{BB} = \frac{0.9 \cdot R_B + R_{BL}}{0.95 \cdot k_B} \tag{2}$$

where R_B is the short-circuit resistance of the battery provided by the manufacturer, R_{BL} is the resistance of the connection cable from the battery to the DC bus, k_B is a coefficient set to 1.05 for charged batteries and to 0.9 for low-charged batteries. The battery voltage before and during the fault is set to the rated voltage of the DC microgrid.

The DC motor resistance is simply the resistance of the DC circuit from the output terminal of the motor and the DC bus.

In the case of a shunt capacitor with rated capacity C, the equivalent resistance of the source is given by:

$$R_{CB} = \frac{R_{CL}}{k_C} \tag{3}$$

where R_{CL} is the resistance of the connection cable from the capacitor to the DC bus and k_C is a coefficient given by IEC 61660 and dependent on the inductance L_{CL} of the same connection cable and on the frequency $\omega_o = 1/\sqrt{L_{CL}C}$. This resistance can be used for calculating the peak value of the short-circuit current, but for steady-state contribution the resistance must be set to infinity.

Finally, in the case of rectifier, the equivalent resistance of the source must consider the contribution of the AC grid upstream of the converter. Using the expressions in IEC 61660, the following resistance can be obtained:

$$R_{CONV} = \frac{1}{c}\left(\sqrt{\frac{2}{3}} \cdot \pi \cdot \frac{Z_Q}{\lambda_d} + R_{loss} + R_{RL}\right) \tag{4}$$

where Z_Q is the module of the short-circuit impedance of the AC grid at the input terminals of the rectifier referred to the DC-side voltage, calculated, according to IEC 60909 by neglecting the presence of the rectifier as a possible element for creating a reclosing loop during the fault on the AC side; λ_d is a coefficient provided by IEC 61660, whose value depends on the rate between the real and imaginary part of Z_Q and the rate between the resistance of the DC circuit downstream of the converter and the resistance of the AC circuit upstream of the converter; R_{loss} is an additional resistance that takes into account the internal power losses of the converter; and R_{RL} is the resistance of the connecting cable from the rectifier to the DC bus. Finally, in (4) the coefficient c is the voltage factor defined by IEC 60909, which is herein introduced to simplify the calculations.

Based on the same principle, it is possible to propose a similar approach for taking into account the presence of PV generators in the calculations. In DC microgrids, PV plants are connected directly to the DC bus or by a DC/DC converter and in both cases their contribution to the short-circuit current is always known and provided by the PV module manufacturer.

Since a photovoltaic field is composed of strings of modules connected in parallel, the short-circuit contribution I_{SC} of a PV plant with N_S strings during a fault in the DC microgrid can be expressed as:

$$I_{SC} = N_S \cdot I_{SC,mod} \tag{5}$$

where $I_{SC,mod}$ is the short-circuit current of a single PV module provided by the manufacturer. With the goal of calculating the maximum short-circuit current in the DC network, it is possible to define an equivalent short-circuit resistance of the PV field so that to also integrate this source in the proposed methodology:

$$R_{FV} = \frac{U_{out}}{I_{SC}} + R_{FL} \tag{6}$$

where U_{out} is the voltage at the output voltage of the PV plant, assumed equal to the rated voltage of the DC system and R_{FL} is the resistance of the connection cable from the PV field

to the DC bus.

Using the above defined resistances and the resistances of the DC cables connecting the buses of the DC microgrids, all elements of the matrix $[G_{SC}]$ are known for the specific microgrid and the short-circuit current and the voltages in all buses during the fault are obtained by solving equation (1) written in explicit form:

$$0 = \sum_{k=1}^{N} G_{hk}(U_{0k} - U_{Fk}) \quad \forall h \neq i$$
$$I_{F,i} = \sum_{\substack{k=1 \\ k\neq i}}^{N} G_{ik}(U_{0k} - U_{Fk}) + G_{ii}U_{0i} \tag{7}$$

III. Case Study

The proposed approach is applied to four test microgrids [7]-[8], three of which are parts of the hybrid MV/LV grid of Fig. 3 and one is the more complex grid represented in Fig. 4: an underground station, a smart car parking, a residential area and a port area microgrid. For each microgrid, a DC-side fault is assumed to occur at the main DC bus. The faulted nodes are indicated in Figures 3 and 4 and named:

- N1 for the underground station microgrid;
- N2 for the smart car parking microgrid;
- N3 for the residential area microgrid;
- N4 for the port area microgrid.

The figures show the state (i.e., open/close) of the AC lines since their state impacts the value of the impedance Z_Q in equation (4). According to the proposed methodology, the initial symmetrical short-circuit powers defined by IEC 60909 at the rectifiers input terminals, necessary for the Z_Q evaluation, are reported in Figures 3 and 4. The four short-circuit currents are calculated considering the contribution of the PV plants and, where present, the contribution of the batteries of electric vehicles connected to the grid. Capacitors and DC motors are not present in any bus of the hybrid grids.

The parameters for the calculation are reported in Tables I through IV. The four tables report all the data necessary to calculate the expressions (2) to (7). For the AC grid upstream the fault location the rated voltage and the initial symmetrical short-circuit power at the rectifier input terminals are given to calculate the maximum short-circuit current on the AC side and the related equivalent short-circuit impedance. For rectifiers and BESSes, the output voltage, the rated power and the internal resistances are given. BESSes are considered charged for the calculation of the maximum short-circuit impedances (i.e., k_b=1.05).

For PV systems also the number of strings N_s and of modules N_m are provided, since the output voltage U_{out} depends on the number of modules connected in series (it is the sum of the output voltage of each series-connected module) and the short-circuit current I_{sc} depends on the number of strings, as expressed by equation (5). For all sources, the length of the connection cables and the related resistances are given; these data are necessary to calculate some of the coefficients appearing in the resistances in the IEC 61660 standard. The Neplan 360® project files with the grids in Figures 3 and 4 may be provided upon request by the authors.

A. Underground station microgrid

The microgrid belongs to an underground station with a floor area of 3000 m^2 and an annual passenger inflow of around 5.3 million, as in the case study described in [28]. From the data in Table I, using the formulas in Section II, the following quantities are calculated:

$$Z_Q = \frac{c \cdot {U_n}^2}{S_{cc}} \cdot \left(\frac{U_{DC}}{U_n}\right)^2 = \frac{1.1 \cdot 2^2}{60.8} \cdot \left(\frac{1.5}{2}\right)^2 = 0.0407\ \Omega$$
$$R_{CONV} = \frac{1}{c}\left(\sqrt{\frac{2}{3}} \cdot \pi \cdot \frac{Z_Q}{\lambda_d} + R_{loss} + R_{RL}\right)$$
$$= \frac{1}{1.05}\left(\sqrt{\frac{2}{3}} \cdot \pi \cdot \frac{0.0407}{0.97} + 0.001 + 0.0025\right) = 0.101\ \Omega$$
$$R_{BB} = \frac{0.9 \cdot R_B + R_{BL}}{0.95 \cdot k_B} = \frac{0.9 \cdot 0.2 + 0.025}{0.95 \cdot 1.05} = 0.206\ \Omega$$
$$R_{FV} = \frac{U_{out}}{I_{SC}} + R_{FL} = \frac{1500}{36.3} + 0.011 = 41.32\ \Omega$$

For the short-circuit current calculation in *N1*, the microgrid can be represented by a simple 4-bus network where *N1* is indicated as bus 2 (Fig. 5). The matrix $[G_{SC}]$, obtained using the coefficient of the system of linear equation (7), is:

$$[G_{SC}] = \begin{bmatrix} 9.88 & -9.88 & 0.00 & 0.00 \\ -9.88 & 14.75 & -4.85 & -0.02 \\ 0.00 & -4.85 & 4.85 & 0.00 \\ 0.00 & -0.02 & 0.00 & 0.02 \end{bmatrix}$$

$[G_{SC}]$ is a 4x4 square matrix being four the nodes involved in the calculation. Imposing that the voltage at buses 1, 3 and 4 during the fault are equal to the rated voltage of the microgrid (such hypothesis is realistic, since these voltages are those internal to the DC sources), the fault current obtained by (7) is 22.13 kA. The same current evaluated by Neplan 360® is 21.77 kA. The difference between the two values is, therefore, 1.6%.

B. Smart car parking microgrid

The network under consideration, schematically represented in Fig. 6, includes the supply of roadside services, charging stations for electric vehicles with slow charging and fast charging, and photovoltaic generation with a dedicated storage system. From the data in Table II, similarly to sub-

section *A*, the following quantities are calculated:

$$Z_Q = 0.0489\ \Omega;\quad R_{CONV} = 0.135\ \Omega;\quad R_{BB} = 0.206\ \Omega;$$
$$R_{BB,ev} = 0.181\ \Omega;\ R_{FV} = 41.32\ \Omega$$

For the short-circuit current calculation in *N2*, the microgrid can be represented as a 5-bus network where *N2* is indicated as bus 2. The matrix $[G_{SC}]$, in this case, is a 5x5 matrix:

$$[G_{SC}] = \begin{bmatrix} 7.40 & -7.40 & 0 & 0 & 0 \\ -7.40 & 17.80 & -4.85 & -5.52 & -0.02 \\ 0 & -4.85 & 4.85 & 0 & 0 \\ 0 & -5.52 & 0 & 5.52 & 0 \\ 0 & -0.02 & 0 & 0 & 0.02 \end{bmatrix}$$

and the fault current is 10.68 kA. The same current evaluated by Neplan 360® is 10.90 kA with a difference between the two values of 2%.

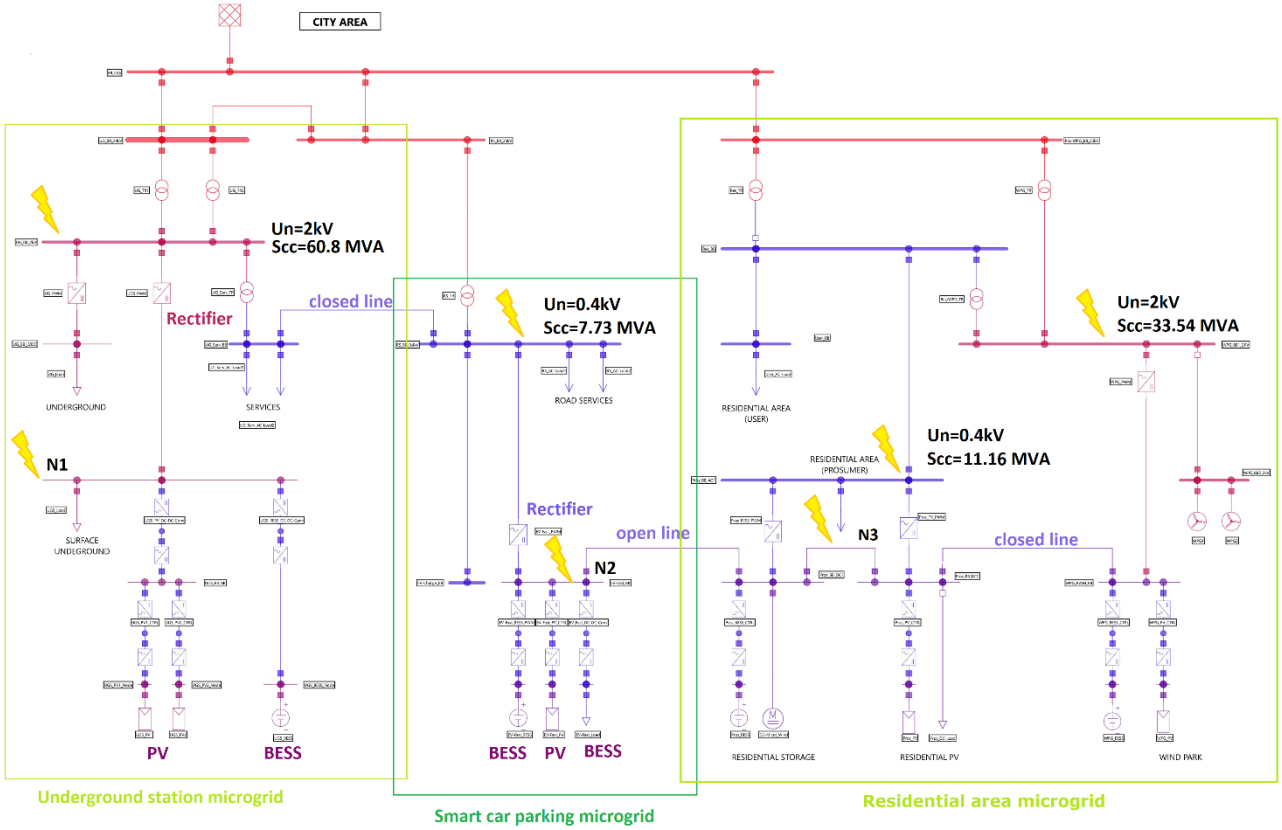

Fig. 3. City area MV/LV AC/DC microgrid.

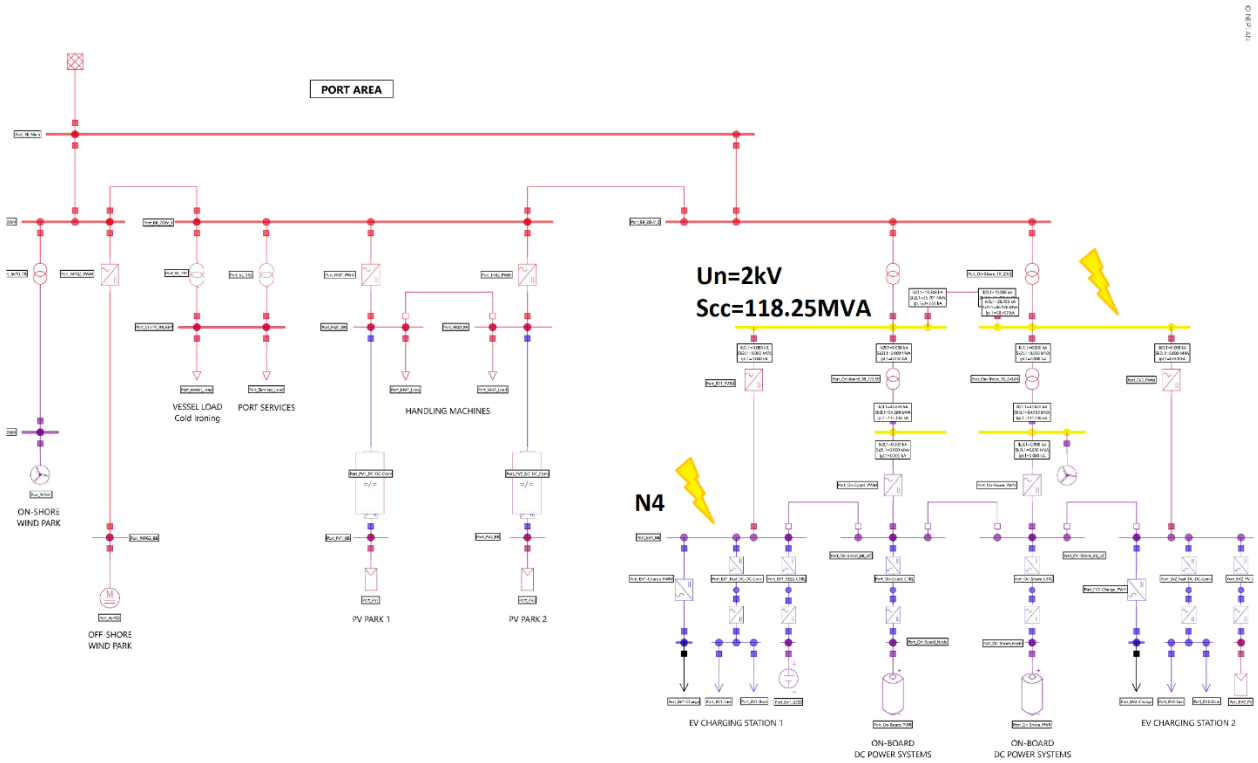

Fig. 4. Port area MV/LV AC/DC microgrid.

TABLE I. UNDERGROUND STATION MICROGRID: PARAMETERS FOR THE CALCULATION OF THE SHORT-CIRCUIT CURRENT.

AC grid	Rated Voltage U_n=2 kV; Initial symmetrical short-circuit power at the input terminals of the rectifier S_{cc}=60.8 MVA
Rectifier	Output Voltage U_{out}=1.5 kV; Rated power S_r=800 kVA; Coefficient λ_d=0.97 (from IEC 61660); Internal resistance R_{loss}=0.001 Ω DC connection cable lenght d=5 m; DC connection cable series resistance R_{RL}=0.0025 Ω
BESS	Output Voltage U_{out}=1.5 kV; Charged battery k_B=1.05; Rated power S_r=250 kVA; Short-circuit resistance of the battery R_B=0.2 Ω; DC connection cable length d=50 m; DC connection cable series resistance: R_{BL}=0.025 Ω
PV	Output Voltage U_{out}=1.5 kV; Number of modules N_m=44; Number of strings Ns=3; Rated power S_r=50 kW; Module's short-circuit current $I_{SC,mod}$=12.1 A; DC connection cable length d=20 m; DC connection cable series resistance R_{FL}=0.011 Ω

TABLE II. SMART CAR PARKING MICROGRID: PARAMETERS FOR THE CALCULATION OF THE SHORT-CIRCUIT CURRENT.

AC grid	Rated Voltage U_n=0.4 kV; Initial symmetrical short-circuit power at the input terminals of the rectifier S_{cc}=7.73 MVA
Rectifier	Output Voltage U_{out}=0.6 kV; Rated power S_r=400 kVA; Coeffient λ_d=0.97 (from IEC 61660); Internal resistance R_{loss}=0.01 Ω DC connection cable length d=5 m; DC connection cable series resistance R_{RL}=0.0025 Ω
BESS	Output Voltage U_{out}=0.6 kV; Charged battery k_B=1.05; Rated power S_r=40 kVA; Short-circuit resistance of the battery R_B=0.2 Ω; DC connection cable length d=20 m; DC connection cable series resistance R_{BL}=0.011 Ω
EV BESS	Output Voltage U_{out}=0.4 kV; Charged battery k_B=1.05; Rated power S_r=400 kVA; Short-circuit resistance of the battery $R_{B,ev}$=0.2 Ω; DC connection cable length d=20 m; DC connection cable series resistance $R_{BL,ev}$=0.0007 Ω
PV	Output Voltage U_{out}=1.5 kV; Number of modules N_m=44; Number of strings Ns=3; Rated power S_r=50 kW; Module's short-circuit current $I_{SC,mod}$=12.1 A; DC connection cable length d=20 m; DC connection cable series resistance: R_{FL} =0.011 Ω

TABLE III. RESIDENTIAL AREA MICROGRID: PARAMETERS FOR THE CALCULATION OF THE SHORT-CIRCUIT CURRENT.

AC grid	Rated Voltage U_{n1} =2 kV Rated Voltage U_{n2}=0.4 kV Initial symmetrical short-circuit power at the input terminals of the rectifier S_{cc1}=33.54 MVA Initial symmetrical short-circuit power at the input terminals of the rectifier S_{cc1}=11.16 MVA
Rectifier (2 kV)	Output Voltage U_{out}=0.6 kV; Rated power S_r=2000 kVA; Coefficient λ_d=0.97 (from IEC 61660); Internal resistance R_{loss}=0.01 Ω DC connection cable length d=5 m; DC connection cable series resistance R_{RL}=0.0025 Ω
Rectifier (0.4 kV)	Output Voltage U_{out}=0.6 kV; Rated power S_r=2x400 kVA; Coefficient λ_d=0.97 (from IEC 61660); Internal resistance R_{loss}=0.01 Ω DC connection cable length d=5 m; DC connection cable series resistance R_{RL}=0.0025 Ω
BESS	Output Voltage U_{out}=0.6 kV; Charged battery k_B=1.05; Rated power S_r=200 kVA; Short-circuit resistance of the battery $R_{B,ev}$=0.2 Ω; DC connection cable length d=20 m; DC connection cable series resistance R_{BL}=0.011 Ω
PV	Output Voltage U_{out}=0.6 kV; Number of modules N_m=1111; Number of strings Ns=52; Rated power S_r=500 kW; Module's short-circuit current $I_{SC,mod}$=189 A; DC connection cable length d=20 m; DC connection cable series resistance: R_{FL} =0.011 Ω

TABLE IV. PORT AREA MICROGRID: PARAMETERS FOR THE CALCULATION OF THE SHORT-CIRCUIT CURRENT.

AC grid	Rated Voltage U_n=2 kV; Initial symmetrical short-circuit power at the input terminals of the rectifier S_{cc}=118.25 MVA
Rectifier (2 kV)	Output Voltage U_{out}=0.69 kV; Rated power S_r=3000 kVA; Coefficient λ_d=0.97 (from IEC 61660); Internal resistance R_{loss}=0.01 Ω DC connection cable length d=5 m; DC connection cable series resistance R_{RL}=0.0025 Ω
On-board BESS	Output Voltage U_{out}=0.69 kV; Charged battery k_B=1.05; Rated power S_r=2x10 MVA; Short-circuit resistance of the battery R_B=0.1 Ω; DC connection cable length d=20 m; DC connection cable series resistance R_{BL}=0.011 Ω
PV	Output Voltage U_{out}=0.69 kV; Number of modules N_m=888; Numero di stringhe Ns=42 Potenza nominale S_r=400 kW Lunghezza del cavo di collegamento in DC d=20 m Resistenza del cavo di collegamento in DC RFL= 0.011 Ω
EV BES	Output Voltage U_{out}=0.69 kV; Charged battery k_B=1.05; Rated power S_r=2000 kVA; Short-circuit resistance of the battery $R_{B,ev}$=0.2 Ω; DC connection cable length d=20 m; DC connection cable series resistance $R_{BL,ev}$=0.0007 Ω

C. *Residential area microgrid*

For the purpose of calculating the short-circuit current at fault point N2, the Residential area microgrid is shown in Fig. 7, where the collecting bus 2 represents the faulted node N3.

From the data in Table III, the following parameters for the solution of the system of linear equation in matrix form in equation (7) are calculated:

$$Z_{Q1} = 0.0113\ \Omega;\ Z_{Q2} = 0.0339\ \Omega;\ R_{CONV1} = 0.097\ \Omega;$$
$$R_{CONV2} = 0.042\ \Omega;\ R_{BB} = 0.181\ \Omega;\ R_{FV} = 0.79\ \Omega$$

The matrix $[G_{SC}]$ in this case is:

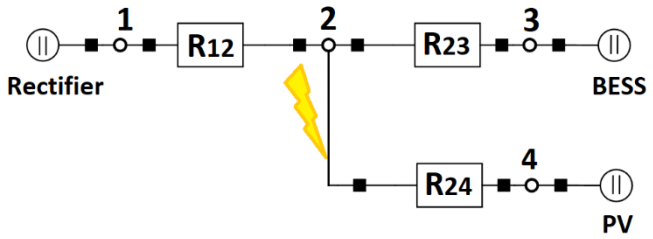

Fig. 5. Schematic representation of the Underground station microgrid.

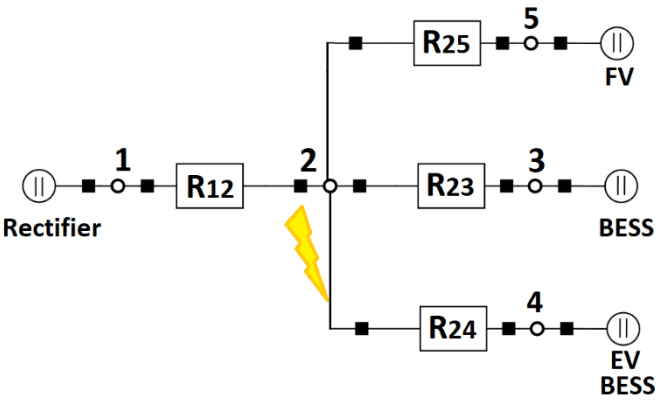

Fig. 6. Schematic representation of the Smart car parking microgrid.

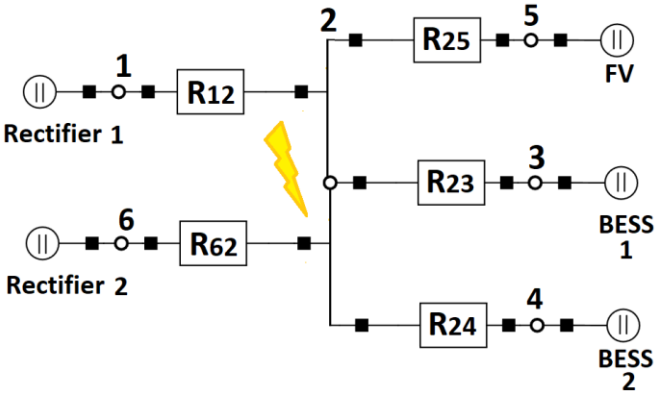

Fig. 7. Schematic representation of the Residential area microgrid.

$$[G_{SC}] = \begin{bmatrix} 10.28 & -10.28 & -5.52 & -5.52 & -1.27 & -24.23 \\ -10.28 & 47.41 & 0 & 0 & 0 & 0 \\ -5.52 & 0 & 5.52 & 0 & 0 & 0 \\ -5.52 & 0 & 0 & 5.52 & 0 & 0 \\ -1.27 & 0 & 0 & 0 & 1.27 & 0 \\ -24.23 & 0 & 0 & 0 & 0 & 24.23 \end{bmatrix}$$

and the fault current obtained from the resolution of equation (7) is 29.50 kA versus 29.13 kA evaluated by Neplan 360®. The difference between the two values is 1.3%.

D. Port area microgrid

Fig. 4 shows a Port Area microgrid. The DC fault point is indicated as N4. The network configuration has two rectifiers in parallel fed from the 2 kV busbars and another two rectifiers fed from the 0.69 kV busbars. When the fault occurs, it is possible to assume that the two rectifiers connected to the 2 kV busbars operate as a single element connecting the DC busbars with the AC busbars. In fact, the formulae proposed by IEC 61660 do not consider the rated power of the rectifier but only its presence. Therefore, since the two elements connect the fault node to the same source, they can be treated as a single element. The presence of the two rectifiers on the 0.69 kV busbars can be instead neglected. In fact, when the fault occurs, the rectifiers fed from the 2 kV busbars create a preferential path for the fault current compared to that formed by the 0.69 kV rectifiers and the 2/0.69 kV/kV transformers in the figure.

Consequently, the network can be represented as in Fig. 8 where node 2 represents fault node N4.

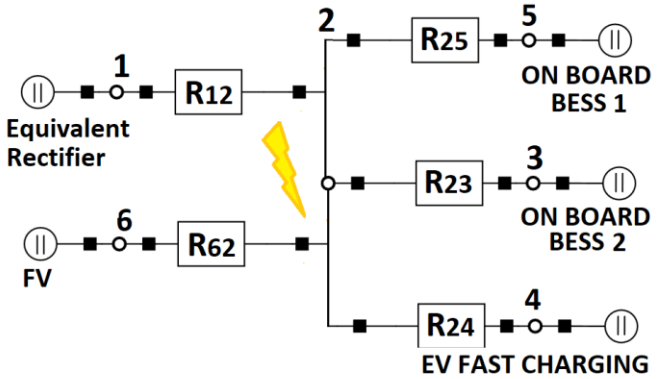

Fig. 8. Schematic representation of the Port area microgrid.

From Data in Table IV the following parameters are calculated:

$$Z_Q = 0.0042\ \Omega;\quad R_{CONV} = 0.024\ \Omega;\quad R_{BB,onboard12} = 0.091\ \Omega;\quad R_{BB,EV} = 0.181\ \Omega;\quad R_{FV} = 1.12\ \Omega$$

and, as a consequence:

$$[G_{SC}] = \begin{bmatrix} 42.23 & -42.23 & -10.99 & -10.99 & -5.52 & -0.89 \\ -42.23 & 70.63 & 0 & 0 & 0 & 0 \\ -10.99 & 0 & 10.99 & 0 & 0 & 0 \\ -10.99 & 0 & 0 & 10.99 & 0 & 0 \\ -5.52 & 0 & 0 & 0 & 5.52 & 0 \\ -0.89 & 0 & 0 & 0 & 0 & 0.89 \end{bmatrix}$$

Even in this case, bus voltages at nodes 1, 3, 4, 5 and 6 are assumed equal to the rated one at the DC side, therefore, from equation (7) a short-circuit current equal to 51.72 kA is obtained. The same current assessed by Neplan 360® is 49.79 kA, with a difference of 3.9% between the two values.

IV. Conclusion

This paper is an extended version of [29], presenting a general methodology for short-circuit calculations in hybrid AC/DC microgrids. The proposed approach shows great accuracy and proves to be easy to apply in all cases where there is no specialized software for the calculation of short-circuit currents in hybrid DC microgrid. The matrix approach lends itself to an iterative implementation that is fairly simple to implement and easily automated. In addition, it allows to consider in a simple way also the presence of PV generators connected to DC buses crossing the limits of IEC 61660 standard.

The computational burden required by this methodology is that necessary for solving a *nxn* linear system and, as shown by the four different case studies, the accuracy of the solution does not change with the increase in the number of nodes of the networks. As to this aspect, the chosen case studies have from 4 to 6 nodes; in real-life microgrids a higher number of sources which can feed the fault are hardly expected, since the control of numerous distributed resources would be rather complex and impractical.

The method can be still improved and simplified by considering the additional indications of IEEE Standard 946-2020 [30]. As an example, according to [22], the contribution of DC motors and inductive loads to the short-circuit current can be conservatively estimated as ten times the motor's rated full-load current. This allows to eliminate from the microgrid graphs those nodes containing DC motors and inductive loads. In this way their fault contribution can be taken into account by adding it to the fault current calculated in the network without these elements, as similarly suggested for AC networks by IEC 60909. In a future work, this methodology will be applied considering the above-mentioned sources and new sources such as fuel cells and Li-ion (or other type of) batteries. In particular, in this case, it will be important to model the contribution of the static converter that interfaces the element to the DC grid.

Finally, a short note to promote a discussion on the topic of short-circuit calculation in DC grids: does the method provided by the IEC 61660 lead to the calculation of significant values of the short-circuit currents in modern smart grids with static converters with current limiters? This is a very important topic

if the age of the standard is considered. Indeed, while smart grids are becoming more and more common in modern distribution systems, the number of static converter-interfaced distributed resources is increasing. It appears rather unrealistic to base the sizing of circuit-breakers and other components on short-circuit current values calculated according to the assumption of the IEC 61660: the effect of current limiters is neglected. This issue may lead to oversizing the ratings of protective devices and it should be discussed by the experts.

ACKNOWLEDGMENT

This research was funded by the Research Fund for the Italian Electrical System under the Contract Agreement "Accordo di Programma 2022-2024" between ENEA and the Ministry of Ecological Transition.

REFERENCES

[1] T. Dragicevic, X. Lu, J. C. Vasquez, J. M. Guerrero, "DC Microgrids—Part I: A Review of Power Architectures, Applications, and Standardization Issues", IEEE Transactions on Power Electronics, Vol. 31, No. 5, 2016, pp. 3528-3549.

[2] T. Dragicevic, X. Lu, J. C. Vasquez, J. M. Guerrero, "DC Microgrids—Part I: A Review of Control Strategies and Stabilization Techniques", IEEE Transactions on Power Electronics, Vol. 31, No. 7, 2016, pp. 4876-4891.

[3] S. Pannala, N. Patari, A. K. Srivastava, N. P. Padhy, "Effective Control and Management Scheme for Isolated and Grid Connected DC Microgrid", IEEE Transactions on Industry Applications, Vol. 56, No. 6, 2020, pp. 6767-6780.

[4] V. Boscaino, J. M. Guerrero, I. Ciornei, L. Meng, E. Riva Sanseverino, G. Zizzo, "Online optimization of a multi-conversion-level DC home microgrid for system efficiency enhancement", Sustainable Cities and Society, Vol. 35, 2017, pp. 417-429.

[5] V. Narayanan, S.a Kewat, B. Singh, "Solar PV-BES Based Microgrid System With Multifunctional VSC", IEEE Transactions on Industry Applications, Vol. 56, No. 3, 2020, pp. 2957-2967.

[6] J. Khodabakhsh, G. Moschopoulos, "Simplified Hybrid AC–DC Microgrid With a Novel Interlinking Converter", IEEE Transactions on Industry Applications, Vol. 56, No. 5, 2020, pp. 5023-5034.

[7] A. Bonì, S. Favuzza, M. G. Ippolito, F. Massaro, S. Modari, R. Musca, V. Porgi, G. Zizzo, "A Simulation Analysis for Assessing the Reliability of AC/DC Hybrid Microgrids – Part I: Underground Station and Car Park", IEEE EEEIC/I&CPS Europe 2021, Bari (Italy), 7-10 Sept. 2021.

[8] A. Bonì, S. Favuzza, M. G. Ippolito, F. Massaro, S. Modari, R. Musca, V. Porgi, G. Zizzo, "A Simulation Analysis for Assessing the Reliability of AC/DC Hybrid Microgrids – Part II: Port Area and Residential Area", IEEE EEEIC/I&CPS Europe 2021, Bari (Italy), 7-10 Sept. 2021.

[9] IEC 61660 series, Short-circuit currents in d.c. auxiliary installations in power plants and substations, IEC, 1997.

[10] S. Skok, S. Tesnjak, S. Stefan, "Transient analysis of auxiliary DC installations in power plants and substations", 2004 IEEE/PES Transmision and Distribution Conference and Exposition: Latin America, Sao Paulo (Brazil), 8-11 Nov. 2004, pp. 1-4.

[11] A. Vicenzutti, E. De Din, G. Sulligoi, "Transient short circuit analysis in DC on-board distribution systems fed by synchronous generators through 6-pulse diode rectifiers", 2015 International Conference on Electrical Systems for Aircraft, Railway, Ship Propulsion and Road Vehicles (ESARS), Aachen (Germany), 3-5 March 2015, pp. 1-6.

[12] A. Vicenzutti, G. Sulligoi, R. Cuzner, V. Singh, "Simplified Analytical Modeling and Experimental Validation of Diode Bridge Rectifier Operation during Rail-to-Rail Short-Circuit Faults in Synchronous Generator-Fed DC Distribution Systems", 2017 IEEE Second International Conference on DC Microgrids (ICDCM), 27-29 June 2017, Nuremburg (Germany).

[13] R. Bleilevens, A. Moser, "Algebraic Modelling of Converters without DC Fault Ride-Through Capability for Short Circuit Current Calculation of DC Distribution Grids", 2018 53rd International Universities Power Engineering Conference (UPEC), Glasgow (UK), 4-7 Sept. 2018, pp. 1-6.

[14] A. Wasserrab, G. Balzer, "Calculation of Short Circuit Currents in HVDC Systems", 2011 46th International Universities' Power Engineering Conference (UPEC), Soest (Germany), 5-8 Sept. 2011, pp. 1-6.

[15] J. C. Das, "Arc-Flash Hazard Calculations in LV and MV DC Systems—Part I: Short-Circuit Calculations", IEEE Transactions on Industry Applications, Vol. 50, No. 3, May-June 2014, pp. 1687-1697.

[16] N. M. R. Santos, V. F. Pires, J. F. Silva "The HVDC Dual Transmission System Under DC Short-Circuit Faults", 2019 IEEE 28th International Symposium on Industrial Electronics (ISIE), 12-14 June 2019, Vancouver (Canada).

[17] P.V. Radu, M. Lewandowski, A. Szelag, M. Steczek, "Short-Circuit Fault Current Modeling of a DC Light Rail System with a Wayside Energy Storage Device", Energies, Vol. 15, 2022, article 3527.

[18] EN 50123-1, Railway applications - Fixed installations - D.C. switchgearPart 1: General, CENELEC, 2003.

[19] S. Wang, G. Zheng, Y. Zhao, W. Zhang, X. Li, "Single-ended Protection Scheme For VSC-HVDC Grids Based On High-Frequency Component Of Fault Current", Journal of Applied Science and Engineering, Vol. 26. Feb 2022.

[20] I. Almutairy, M. Alluhaidan, "Protecting a low voltage DC microgrid during short-circuit using solid-state switching devices", 2017 IEEE Green Energy and Smart Systems Conference (IGESSC), 6-7 Nov. 2017, Long Beach (USA).

[21] L. Yixiang, W. Xiangheng, W. Shanming, S. Pengsheng, M. Weiming, "Analysis of the DC side sudden short circuit of three-phase/twelve-phase synchronous generator system", PowerCon 2000. 2000 International Conference on Power System Technology, 4-7 Dec. 2000, Perth (Australia).

[22] S. Moussa, M. J. B. Ghorbal, J. A. Ziani, I. Slama-Belkhodja, "Residual-based Short-Circuit fault detection and isolation in LVDC microgrid", Sustainable Energy Technologies and Assessments, Vol. 54, 2022, article 102803.

[23] S. Yuan, J. Yan, Y. Yu, C. Zhao, G. Su, X. Li, "Calculation method of short-circuit fault current in flexible DC grid", Energy Reports, Vol. 8, 2022, pp. 461-468.

[24] A. Wasserrab, G. Balzer, "Calculation of short circuit currents in HVDC systems" in Proc. 46th Int. Conf. Univ. Power Eng., 2011, pp. 1–6.

[25] B. Li, X. Jiao, W. Wen, W. Wang, B. Li, "Study on Calculation Method for Steady-state Short-circuit Current of MMC during a DC pole-to-pole Fault", IEEE Transactions on Power Delivery, Vol. 37, No. 4, 2022, pp. 2492-2502.

[26] X. Feng, L. Qi, Z. Wang, "Estimation of short circuit currents in mesh DC networks", 2014 IEEE PES General Meeting | Conference & Exposition, National Harbor, MD (USA), 27-31 July 2014, pp. 1-5.

[27] V. Cataliotti, "Electrical Installations" (*In Italian*), Flaccovio, Palermo (Italy), 1998.

[28] L. Lin, X. Liu, T. Zhang, X. Liu, "Energy consumption index and evaluation method of public traffic buildings in China", Sustainable Cities and Society, 2020, vol. 57, article 102132.

[29] S. Favuzza, M. Mitolo, R. Musca, G. Zizzo, "Short-circuit Calculations in Hybrid AC/DC Microgrids", 2022 IEEE/IAS 58th Industrial and Commercial Power Systems Technical Conference (I&CPS), Las Vegas (USA), 2-5 May 2022.

[30] IEEE Standard 946-2020, "IEEE Recommended Practice for the Design of DC Power Systems for Stationary Applications".